13.2, 13.3 Received 24 August 1970

Focusing and Refraction of Harmonic Sound and Transient Pulses in Stratified Media

D. A. SACHS AND A. SILBIGER*

Cambridge Acoustical Associates, Incorporated, Cambridge, Massachusetts 02138

In media for which the speed of sound is position dependent, propagating sound will be refracted and, in some cases, focused. In the focusing regions, usually referred to as caustics or convergence zones, significant amplification of the pressure levels above those predicted by spherical spreading has been observed for continuous waves as well as for explosive pulses. In addition, the waveforms of explosive pulses undergo drastic distortion. In the present paper, an asymptotic theory of the refraction and focusing of sound originating from a point source in a stratified medium is presented. It is applicable to realistic velocity profiles and encompasses both transient pulses and harmonic waves. A comparison with Barash's and Goertner's recent experiment involving explosive pulses indicates that the theory gives reliable estimates of the peak pressure levels at caustics, but reproduces only qualitatively the shape of the focused pulse. The discrepancy is attributed mainly to the neglect of finite-amplitude effects in the theory's formulation. The inaccuracies inherent in the high-frequency asymptotic methods employed in the theory are discussed in some detail.

INTRODUCTION

Because the speed of sound varies from point to point in most bodies of water, propagating sound energy does not travel in straight lines but rather is refracted into curved paths. Under certain conditions, the paths will converge and sound energy that had previously been distributed over a large volume is focused into a narrow region. The formation of these focusing regions—called caustics or convergence zones—is easy to visualize in the ray picture of geometric acoustics. Consider a converging bundle of rays. The cross-sectional area of the bundle evidently diminishes in the direction of propagation, and eventually the focal point may be reached where the cross-section vanishes. Ordinarily the focal points of adjacent ray bundles do not coincide, but lie on a surface called the caustic. In special cases, the focal points do coalesce. Since in ray theory the intensity along a ray is inversely proportional to the cross-sectional area of the ray bundle, an infinite intensity would be predicted at the focus. For finite nonzero wavelengths, the focus can only be defined as a region with a high concentration of energy; only in the short wavelength limit where ray theory is rigorously valid will this region shrink to a point at which an infinite intensity is predicted. Experimentally, Barash and Goertner[1] have observed peak pressures over five times the values expected for isovelocity water for underwater explosion shock waves; at the same time, the width of the focused pulse was reduced by a factor of 3 or more compared to that of unrefracted pulses. The maximum pressures are generally found in the regions where ray theory predicts the formation of caustics.

In this paper, the refraction and focusing of waves originating from a point source in a stratified medium is considered, the ultimate objective being the explanation of experimental data on the behavior of underwater explosive shock waves at caustics. While there is a large amount of literature in optics concerning caustics (primarily restricted to waves in homogeneous media), the consideration of caustics in underwater sound is relatively new (since about 1941), and most of the published work on the subject has been devoted to harmonic sources and to specific models of the propagating medium.[2–9] Mathematical treatments of caustics, mostly confined to steady-state sources, are given in Refs. 10–12. We extend present theories along two lines. Drawing upon the procedures presented by Seckler and Keller,[13] we present a generalized formulation applicable to arbitrary sound-velocity profiles, for which both the source and the caustic may be contained in a nonhomogeneous region. Secondly, in addition to harmonic waves, we consider transient pulses and, in particular, explosive-type signals.

The formulation is based on the fundamental assumption that nonlinear effects may be neglected. In regions away from caustics, the theory is equivalent to geometrical acoustics. However, in the vicinity of caustics, geometrical acoustics is not valid, but through the use of a higher-order approximation, the theory yields predictions on the caustic itself and in the nearby shadow zone, for time-harmonic waves. Nevertheless, for explosive pulses, the theory again predicts an infinite intensity at caustics, which suggests that linear acoustics itself may be invalid in focal regions.[14] The most satisfying way to remedy this defect would be to introduce finite-amplitude effects directly into the theory, but, up to the present, the mathematical complexities of this task have not been overcome. In the hope, however, that some sort of correspondence to reality will be achieved, viscous dissipation, which is known to exist experimentally and which can be handled mathematically, is incorporated into the theory to ensure finite pressure levels.

A comparison of theoretical predictions with the results of an experiment involving explosive pulses indicates that reasonable predictions of peak pressure levels at caustics can be obtained with the neglect of nonlinear effects. The fact that the waveform of the focused pulse is predicted only qualitatively is probably due to the omission of finite-amplitude effects from the theoretical framework. In general, since the theory is based on the linear acoustics approximation, it is certainly not expected to yield valid results for large-amplitude pressure waves. Nevertheless, the present theory can be viewed as a necessary first step towards a more comprehensive formulation incorporating nonlinear effects, and work towards this end is currently in progress.

It is plausible, however, that nonlinear and refractive phenomena may, to some extent, act independently so that their effects on a propagating wave may be linearly superposed. A method based on this point of view is described in an accompanying paper by Blatstein.[15] It uses the present theory in conjunction with the empirically valid similitude equations[16] (which include finite-amplitude effects) and, in effect, accounts for nonlinearities during the propagation of the explosive pulse to the caustic vicinity (but ignores them at the caustic itself). The method shows good correlation with the results of experiments involving large explosives and great propagation ranges, and is partially successful in short-range experiments.

The present paper is divided into four parts. In Sec. I, the theory of refraction and focusing phenomena from a harmonic source is evolved. Equation 14, the central result of Sec. I, gives the pressure at and in the vicinity of a caustic. In Sec. II, these results are used to describe focusing and refraction phenomena from a transient source by means of Fourier transformation. Equation 25 gives the time-dependent field in the caustic vicinity. In Sec. III, predictions of the theory are compared with some experimental results collected recently in a flooded quarry by Barash and Goertner (see Fig. 13). In Sec. IV, the results of the paper are summarized and some conclusions discussed. Details of the theoretical development not given here can be found in Refs. 17 and 18.

I. REFRACTION AND FOCUSING FROM A HARMONIC SOURCE

We obtain a high-frequency solution for a harmonic point source in a refractive medium. This asymptotic solution is the same as ray acoustics and gives rise to an infinite pressure at a caustic. Consequently, a higher-order approximation is obtained for which the pressure remains finite. The accuracy of the approximation is then discussed. Finally, some examples are given that illustrate the application of the theory and also give some further insight into its domain of validity.

A. General Solution for a Point Source

We consider a medium whose sound speed varies in the vertical direction, which we take to coincide with the z axis of a Cartesian coordinate system (x,y,z). For brevity, we assume that there is no water surface or bottom interface present. We assume a sound source at the origin that emits an initially spherical harmonic wave,

$$p(R,t)\approx\frac{P\exp[-i\omega(t-R/c)]}{(4\pi R)}\quad(R\approx 0),$$

where R is the radial distance from the source to the observation point. We must find solutions to the reduced wave equation

$$\nabla^2p+k^2n^2(z)p=-P\delta(x)\delta(y)\delta(z),\tag{1}$$

where p is the pressure field, $n(z)$ is the index of refraction normalized at the source

$$n(z)=c(0)/c(z),$$

$c(z)$ is the sound speed (a function of z), and k is the wavenumber at the source

$$k=\omega/c(0).$$

(The time-dependence factor $e^{-i\omega t}$ has been suppressed in Eq. 1 and is omitted in the following.)

Because the problem is cylindrically symmetric around the z axis, it is convenient to introduce the cylindrical coordinate system (r,ϑ,z), where r is the radial distance in the horizontal direction and ϑ is the azimuthal angle in the horizontal plane. By applying a Hankel transform,[19] Eq. 1 can be reduced to an ordinary differential equation:

$$\partial^2f/\partial z^2+k^2[n^2(z)-\xi^2]f=-(P/2\pi)\delta(z),\tag{2}$$

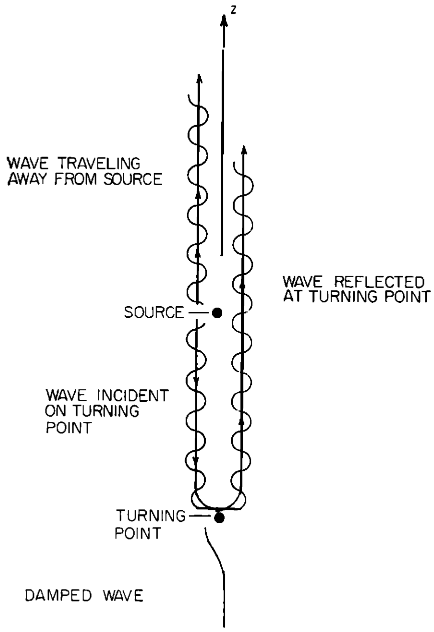

FIG. 1. Schematic representation of the WKB solutions in the presence of a turning point.

where the Hankel transform of p is defined by

$$f(\xi,z)=\int_0^\infty p(r,z)J_0(k\xi r)rdr,$$

and the inverse transform is given by

$$p(r,z)=\int_0^\infty f(\xi,z)J_0(k\xi r)k^2\xi d\xi.$$

The path of integration in the inverse transform can be extended to include the entire ξ axis by following a standard procedure.[20] We obtain

$$p(r,z)=\frac{1}{2}\int_{-\infty}^{+\infty} f(\xi,z)H_0^{(1)}(k\xi r)k^2\xi d\xi.$$

We can consider this integral a superposition of partial waves which, in regions at distances from the source large compared to a wavelength and for which n does not vary appreciably over a wavelength, appear over localized regions as being approximately of the form

$$A(\xi,r,z)\exp[ik\xi r+ik(n^2-\xi^2)^{\frac{1}{2}}z].$$

For $\xi<n$, such terms resemble plane waves propagating at an angle $\sin^{-1}(\xi/n)$ with the z axis. Those terms with $\xi>n$ decrease exponentially in the z direction (inhomogeneous waves), and their contribution to the integral will be small for large kz.

For the present we need only concern ourselves with the nature of the integrand in ranges of ξ where $\xi<n$, since the behavior in this region largely governs the form of the wave. The range of such values of ξ varies with z; at the source, where $z=0$, we accordingly consider $\xi<1$.

For a specific ξ, there may exist points z_T at which $n(z_T)=\xi$. Such points are called the turning points of differential equation, Eq. 2. The propagation angle $\sin^{-1}(\xi/n)$ becomes horizontal and the vertical component of the wave's motion reverses its direction. It is shown that corresponding to each reflection at a turning point, at most, one caustic is formed. We study the formation of a caustic, after reflection at the first turning point. Reflections from further turning points will be ignored.

B. The WKB Solution

An exact solution of Eq. 2 is only possible for certain simple analytical forms of $c(z)$. However, a general high-frequency asymptotic solution can be given with the aid of the WKB approximation.[21] We assume in the following that a turning point exists and that it lies below the source. This happens if $c(z)$ monotonically decreases with increasing z or, if $c(z)$ is not monotonic, if the existence of a boundary prevents the formation of turning points above the source.

The WKB solutions corresponding to waves that have left the source but have not passed through a turning point are

$$f(\xi,z)=\frac{P\exp\{\pm ik[\varphi(0)-\varphi(z)]+i\pi/2\}}{4\pi k(n^2-\xi^2)^{\frac{1}{4}}(1-\xi^2)^{\frac{1}{4}}},\qquad(3)$$

where the sign in the exponential is taken positive or negative depending on whether z is negative or positive. The WKB solution corresponding to the wave reflected at the turning point (but traveling away from the source in the r direction) is given by

$$f_r(\xi,z)=\frac{P\exp\{ik[\varphi(0)+\varphi(z)]\}}{4\pi k(n^2-\xi^2)^{\frac{1}{4}}(1-\xi^2)^{\frac{1}{4}}}.\qquad(4)$$

The auxiliary function $\varphi(z)$ is defined by

$$\varphi(z)=\int_{z_T}^{z}[n^2(z)-\xi^2]^{\frac{1}{2}}dz.\qquad(5)$$

A schematic picture of the WKB solutions is given in Fig. 1.

C. Ray-Acoustics Solution

The inverse Hankel transform is evaluated asymptotically in the limit of large frequency by means of the method of steepest descents.[22] Substituting for the Hankel function its asymptotic form for large arguments, and for $f(\xi,z)$ the WKB approximations given by Eqs. 3 and 4, we obtain for waves which have left the source (but which have not passed through a turning point)

$$p(r,z)=\frac{P}{4\pi}\int_{-\infty}^{+\infty}d\xi \times\left[\frac{k\xi}{2\pi r(n^2-\xi^2)^{\frac{1}{2}}(1-\xi^2)^{\frac{1}{2}}}\right]^{\frac{1}{2}}e^{ikW(\xi,r,z)+i\pi/4}, \quad (6)$$

where

$$W(\xi,r,z)=\xi r\pm[\varphi(0)-\varphi(z)],$$

and, for the wave reflected at the turning point,

$$p(r,z)=\frac{P}{4\pi}\int_{-\infty}^{+\infty}d\xi \times\left[\frac{k\xi}{2\pi r(n^2-\xi^2)^{\frac{1}{2}}(1-\xi^2)^{\frac{1}{2}}}\right]^{\frac{1}{2}}e^{ikW(\xi,r,z)-i\pi/4}, \quad (7)$$

where

$$W(\xi,r,z)=\xi r+\varphi(0)+\varphi(z). \quad (8)$$

The branch cuts of the square roots in Eqs. 6 and 7 lie along the negative axis, and, for positive real values of the arguments, the positive square root is to be taken.

If $\partial W/\partial\xi$ has zeros at $\xi=\xi_j$, and k is sufficiently large, the method of steepest descents informs us that the main contributions to the integral are in the vicinity of these zeros. We expand $W(\xi)$ around $\xi=\xi_j$:

$$W(\xi)=W_j+\tfrac{1}{2}(\xi-\xi_j)^2W_j''+\cdots, \quad (9)$$

where

$$W_j=W(\xi_j), W_j''=\partial^2W(\xi)/\partial\xi^2|_{\xi=\xi_j}, \text{ etc.}$$

By definition

$$W_j'=0. \quad (10)$$

Assuming the amplitudes in the integrands of Eqs. 6 and 7 are slowly varying in the neighborhood of ξ_j, and neglecting higher-order terms in Eq. 9, we find, provided $W_j''\neq 0$, for the wave incident upon the turning point

$$p_i(r,z)=\frac{P}{4\pi}\sum_j\left\{\frac{\xi_j}{r(1-\xi_j^2)^{\frac{1}{2}}(n^2-\xi_j^2)^{\frac{1}{2}}[\varphi''(0)-\varphi''(z)]}\right\}^{\frac{1}{2}} \times\exp\{ik[\xi_j r+\varphi(0)-\varphi(z)]+i\pi/2\}, \quad (11)$$

and for the reflected wave

$$p_r(r,z)=\frac{P}{4\pi}\sum_j\left\{\frac{\xi_j}{r(1-\xi_j^2)^{\frac{1}{2}}(n^2-\xi_j^2)^{\frac{1}{2}}[\varphi''(0)+\varphi''(z)]}\right\}^{\frac{1}{2}} \times\exp\{ik[\xi_j r+\varphi(0)+\varphi(z)]\}. \quad (12)$$

In writing Eqs. 11 and 12, we have, for brevity, assumed that W_j'' is positive, and we also recall that we are confining ourselves to modes with $\xi_j<n(z)$, 1. Furthermore, with the assumption that $c(z)$ monotonically decreases with increasing height, it can be shown that $\xi_j\geqq 0$.

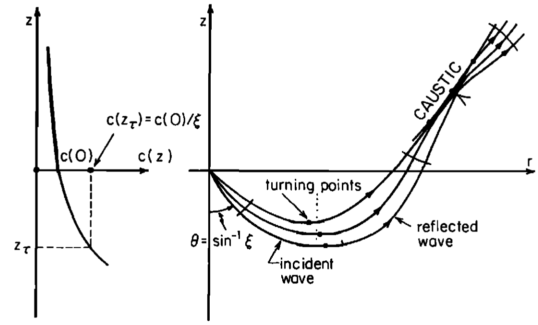

FIG. 2. Ray diagram and velocity profile.

Equations 11 and 12 are equivalent to the ray-acoustics solutions; each term corresponds to a ray leaving the source at an angle $\theta_j=\sin^{-1}\xi_j$ with the vertical (see Fig. 2).

It might appear that Eqs. 11 and 12 are not valid at turning points, where $(n^2-\xi_j^2)^{\frac{1}{2}}$ vanishes. However, as $z\rightarrow z_\tau$, the term $\varphi''(z)$ in the denominator will be found to diverge as $(n^2-\xi_j^2)^{-\frac{1}{2}}$, and hence no singularity appears. Furthermore, since, from Eq. 5, both $\varphi(z)\rightarrow 0$ and $\varphi'(z)\rightarrow 0$ as $z\rightarrow z_\tau$, the phases of Eqs. 11 and 12 become identical at the turning point. [Note that the $\pi/2$ in the phase of Eq. 11 is cancelled by the appearance of an i in the denominator, which arises because $W_j''\rightarrow -(n^2-\xi_j^2)^{-\frac{1}{2}}$ as $z\rightarrow z_\tau$.] Thus the two ray solutions have well-defined bounded *identical* limits at turning points and hence are usable at these points. It therefore follows that there is no phase shift at a turning point (unless the turning point lies on a caustic). The absence of a phase shift at a turning point has been verified in an exactly soluble problem (see Sec. I-E and also Ref. 23); experimental evidence[24] also appears to confirm the same conclusion.

The ray solutions cannot, however, be used at a caustic. Mathematically, a caustic will arise when the denominator in Eqs. 11 or 12 vanishes because W_j'' goes to zero. In the range under consideration (in which $n>\xi_j$), $\varphi''(z)$ is an increasing function of decreasing z. Hence, the denominator in the expression for p_i will have no zeros other than at the origin. However, for increasing z, $\varphi''(z)$ decreases and there may exist a point z at which $\varphi''(z)=-\varphi''(0)$. The location of the caustic is then found from the solution of this equation, which is independent of r, and from Eq. 10, or $r=\varphi'(z)-\varphi'(0)$, where φ is defined in Eq. 5. In differentiation with respect to ξ, it should be kept in mind that the lower limit of integration in Eq. 5 is a function of ξ through the relation $n(z_\tau)=\xi$. The order of integration and differentiation should not be reversed unless this dependence is taken into account.

We conclude that the rays will not encounter a caustic between the source and first turning point, but may pass through at most one caustic after passing the turning point. In other words, only the ray reflected at the turning point (Eq. 12) can pass through a caustic.

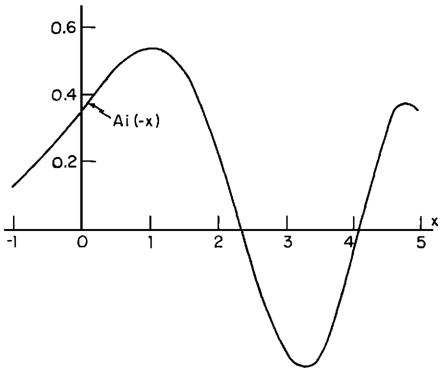

FIG. 3. Airy function.

No second caustic will be encountered unless the rays are reflected again by a second turning point.

D. The Field at a Caustic

Consider some point on the caustic (r_c,z_c). The ray going through this point is given by $\xi=\xi_c$, the solution of $W'(\xi_c,r_c,z_c)=0$. By definition, we also have for a point on the caustic $W''(\xi_c,z_c)=0$. W'' is independent of r (see Eq. 8). Hence, for some point at the same depth but not on the caustic $(r\neq r_c,\ z=z_c)$, we have $W'(\xi_j,r,z_c)=0$ but $W''(\xi_j,z_c)\neq 0$, while at this same point $W'(\xi_c,r,z_c)\neq 0$ but $W''(\xi_c,z_c)=0$.

For points not on the caustic, if we expand $W(\xi)$ around ξ_c, we will automatically get rid of the term in W'':

$$W(\xi,r,z_c)=W_c(r)+W_c'(r)\Delta\xi+\tfrac{1}{6}W_c'''(\Delta\xi)^3,$$

where

$$\Delta\xi\equiv\xi-\xi_c, W_c(r)\equiv W(\xi_c,r,z_c),\cdots\text{etc.}$$

From Eq. 8 it follows that

$$W_c'(r)-W_c'(r_c)=[r+\varphi'(0)+\varphi'(z_c)]-[r_c+\varphi'(0)+\varphi'(z_c)],$$

and, using the fact that $W_c'(r_c)=0$,

$$W_c'(r)=r-r_c=\Delta r.$$

Assuming the amplitude factor in Eq. 7 is slowly varying, the integral becomes

$$p(r,z_c)=\frac{P}{4\pi}\left[\frac{k\xi_c}{2\pi r(n^2(z_c)-\xi_c^2)^{\frac12}(1-\xi_c^2)^{\frac12}}\right]^{\frac12}e^{ikW_c(r)-i\pi/4}\times\int_{-\infty}^{+\infty}e^{i(\pm\rho s+s^3/3)}ds,\quad(13)$$

where

$$s=\Delta\xi\left[\pm k^{\frac13}\left|\frac{W_c'''}{2}\right|^{\frac13}\right],$$

$$\rho=\zeta\Delta r k^{\frac23},$$

and

$$\zeta=(\tfrac12|W_c'''|)^{-\frac13},\quad W_c'''\gtrless 0.$$

The integral can be expressed in terms of the Airy function (Fig. 3), giving

$$p(r,z_c)=\frac{P}{4\pi}k^{1/6}\zeta\left\{\frac{2\pi\xi_c}{r[n^2(z_c)-\xi_c^2]^{\frac12}(1-\xi_c^2)^{\frac12}}\right\}^{\frac12}\times\mathrm{Ai}(\pm k^{\frac23}\zeta\Delta r)e^{ikW_c(r)-i\pi/4},\quad W_c'''\gtrless 0.\quad(14)$$

This solution expresses the field at an arbitrary height z_c as a function of Δr, the horizontal distance from the caustic. The sign of W_c''' is negative if the shadow zone lies between the z axis and the caustic boundary; it is positive if the illuminated zone covers the same region (Fig. 4). The applicability of Eq. 14 is restricted not only to large frequencies, but also to the vicinity of the caustic. It is, however, valid on both sides of the caustic ($\Delta r>0$, $\Delta r<0$) as well as on the caustic itself ($\Delta r=0$). On the caustic, the pressure is seen to increase with the one-sixth power of frequency.

On the illuminated side of the caustic (the positive x axis in Fig. 3), the interference of rays approaching and receding from the caustic produces spatial oscillations in the field amplitude. Note that the peak pressure occurs not on the caustic itself, but at some distance away. In the shadow zone (the negative x axis), the amplitude is strongly damped with distance.

The ray solution for the reflected wave, Eq. 12, becomes inaccurate in the vicinity of the caustic, while the caustic field solution, Eq. 14, is valid only in a region around the caustic. It can be shown[17] that the layer about the caustic in which Eq. 14 rather than the ray solution must be used, is defined by

$$k(\zeta|\Delta r|)^{\frac32}\lessapprox 1.\quad(15)$$

Because Eq. 14 is applicable in a layer centered on the caustic, it is referred to as the "caustic boundary-layer solution."

On the shadow side of the caustic, the roots ξ_j of Eq. 10 are complex. According to geometrical acoustics, this region corresponds to the shadow zone. By the introduction of complex rays, ray theory can be extended to predict nonzero pressures in this region. In the vicinity of the caustic, the caustic boundary-layer solution is still valid.

E. Accuracy of the Caustic Field Solution

A number of approximations have been used to obtain the caustic boundary-layer solution, and it is therefore useful to obtain an estimate of its accuracy.

If we retain the next higher-order terms in the Taylor series expansions of the amplitude factor of Eq. 7 and the phase function, Eq. 9, we have

$$\left[\frac{\xi}{(n^2-\xi^2)^{\frac12}(1-\xi^2)^{\frac12}}\right]=\frac{\xi_c}{(n^2-\xi_c^2)^{\frac12}(1-\xi_c^2)^{\frac12}}+\frac{\partial}{\partial\xi}\left[\frac{\xi}{(n^2-\xi^2)^{\frac12}(1-\xi^2)^{\frac12}}\right]^{\frac12}\Bigg|_{\xi=\xi_c}\Delta\xi\quad(16)$$

and

$$W(\xi)=W_c(r)+W_c'(r)\Delta\xi+(1/6)W_c'''(\Delta\xi)^3 +(1/24)W_c''''(\Delta\xi)^4. \quad (17)$$

Higher-order terms in the asymptotic expansion of the Hankel function and similar higher-order corrections to the WKB solutions can be ignored, since they will lead to terms of much higher order in frequency than those we derive below.

If we imagine that the term involving W_c'''' in Eq. 17 is a small correction, then we may write

$$e^{ikW(\xi)}=\exp\{ik[W_c(r)+\Delta r\Delta\xi+(W_c'''/6)(\Delta\xi)^3]\} \times[1+ik(W_c''''/24)(\Delta\xi)^4]. \quad (18)$$

If we suppose that the term containing $\Delta\xi$ in Eq. 16 is also small, then retaining only lowest-order correction terms, the substitution of Eqs. 16 and 17 into Eq. 7 gives

$$p(r,z_c)=\frac{P}{4\pi}\left(\frac{k}{2\pi r}\right)^{\frac{1}{2}} e^{ikW_c(r)}\int_{-\infty}^{\infty} d\xi e^{ik[\Delta r\Delta\xi+(W_c'''/6)(\Delta\xi)^3]} \times\left[F_c+F_c'\Delta\xi+\frac{ik}{24}F_cW_c''''(\Delta\xi)^4\right], \quad (19)$$

where

$$F(\xi)\equiv[\xi/(n^2-\xi^2)^{\frac{1}{2}}(1-\xi^2)^{\frac{1}{2}}]^{\frac{1}{2}}$$

and

$$F_c=F(\xi_c),\ F_c'=\partial F(\xi)/\partial\xi|_{\xi=\xi_c}.$$

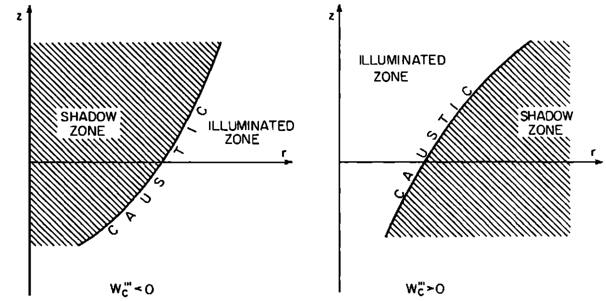

FIG. 4. Relation of shadow-zone location to sign of W_c'''.

By comparison with Eq. 13, the integral of the first term in the square brackets in Eq. 19 is the caustic boundary-layer solution of Eq. 14. The remaining terms can be evaluated by noting that, for the integral

$$I_n\equiv\int_{-\infty}^{+\infty} d\xi e^{ik[\Delta r\Delta\xi+(W_c/6)(\Delta\xi)^3]}(\Delta\xi)^n,$$

a recursion formula

$$I_n=\left(\frac{1}{ik}\frac{\partial}{\partial\Delta r}\right)^n I_{n-1}\ (n=1,2,3,4,\cdots)$$

holds, where

$$I_0=(2\pi\zeta/k^{\frac{1}{3}})\,\mathrm{Ai}(\pm\rho),\quad (W_c'''\lesseqgtr 0).$$

The final result for the pressure is

$$p(r,z_c)=\frac{P}{4\pi}k^{1/6}\zeta\left\{\frac{2\pi\xi_c}{r[n^2(z_c)-\xi_c^2]^{\frac{1}{2}}(1-\xi_c^2)^{\frac{1}{2}}}\right\}^{\frac{1}{2}}\mathrm{Ai}(\pm\rho)e^{ikW_c(r)-i\pi/4}+\frac{P}{4\pi k^{1/6}}\left(\mp\zeta^2\frac{\partial}{\partial\xi}\left\{\frac{2\pi\xi}{r[n^2(z_c)-\xi^2]^{\frac{1}{2}}(1-\xi^2)^{\frac{1}{2}}}\right\}^{\frac{1}{2}}\Bigg|_{\xi=\xi_c} \times\mathrm{Ai}'(\pm\rho)+\frac{\zeta^5}{24}\left\{\frac{2\pi\xi_c}{r[n^2(z_c)-\xi_c^2]^{\frac{1}{2}}(1-\xi_c^2)^{\frac{1}{2}}}\right\}^{\frac{1}{2}}W_c''''[2\,\mathrm{Ai}'(\pm\rho)+\rho^2\,\mathrm{Ai}(\pm\rho)]\right)e^{ikW_c(r)+i\pi/4},\quad (W_c'''\gtrless 0), \quad (20)$$

where

$$\mathrm{Ai}'(\pm\rho)\equiv d\,\mathrm{Ai}(x)/dx|_{x=\pm\rho}$$

and

$$\rho=(\tfrac{1}{2}|W_c'''|)^{-\frac{1}{3}}\Delta r k^{\frac{2}{3}}.$$

Equation 20 expresses the pressure field as the sum of the caustic boundary-layer solution (Eq. 14) and a "correction" term. The correction is to be applied only in the caustic boundary layer defined by Eq. 15. A more complete analysis indicates that the pressure field can be expressed in terms of an asymptotic series,[25] for which Eq. 14 is the leading order term and the correction is the next higher-order term, provided that the quantity ρ is always finite. Because of Eq. 15, this condition is automatically satisfied.

It should be recalled that asymptotic series are radically different from the convergent series usually encountered. For a convergent series, the accuracy of a partial sum can generally be increased by the use of additional terms and the process repeated indefinitely to achieve any desired degree of accuracy. In contrast, for an asymptotic series, the addition of higher order terms to the leading term may at first increase the accuracy of the answer, but eventually a point will be reached where the use of additional higher-order terms will decrease the accuracy.

Although the optimum procedure for using the asymptotic series whose first two terms are given in Eq. 20 has not been determined, a study[25,26] of other asymptotic series suggests that the correction term can be useful in several ways: (1) If the magnitude of the correction term is very small in comparison to the caustic boundary-layer solution, then the latter is an accurate approximation. (2) If, on the other hand, the correction is much larger than the uncorrected term, then the caustic boundary-layer solution is probably very inaccurate. In this instance, an analogous study by Senior[26] suggests to us that the *best possible answer is obtained by using the caustic boundary-layer solution*

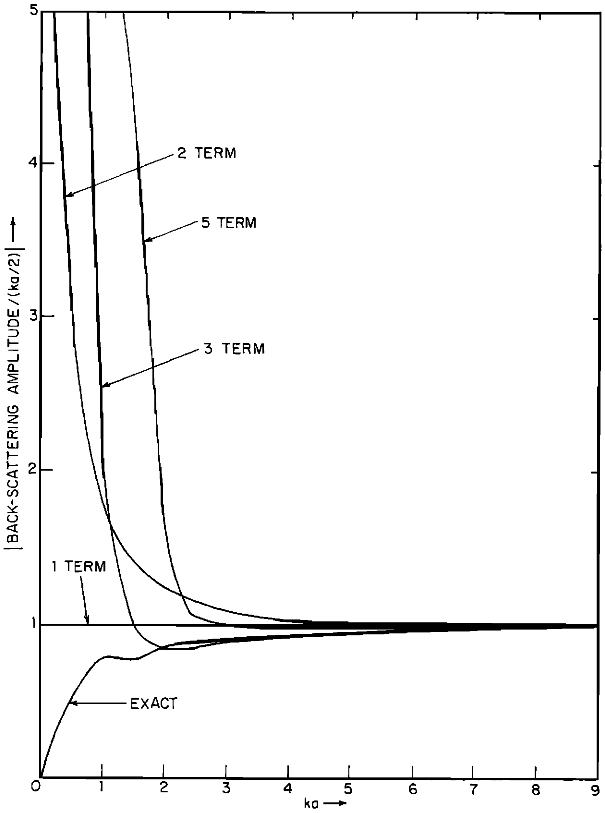

FIG. 5. Comparison of partial sums of an asymptotic expansion with exact answer (adapted from Senior, Ref. 26).

alone. (3) Finally, if Eq. 20 is used to represent the pressure, the result may be more accurate down to lower frequencies than Eq. 14 alone, which tends to become progressively more erroneous as the frequency decreases. Ultimately, however, even Eq. 20 will begin to err drastically for sufficiently low frequencies.

These "rules" governing the use of higher-order terms in an asymptotic expansion are illustrated in one of the problems studied by Senior, the backscattering of plane sound waves by a rigid sphere. For a quantity closely related to the backscattering amplitude, Senior computes the values of an exact series expression and compares them with various partial sums of an asymptotic expansion for the same quantity. The expansion is expressed in inverse powers of ka, where k is the wavenumber and a the radius of the sphere (Fig. 5). In Fig. 5, the curve labeled "1-term" is obtained by retaining only the leading-order term of the asymptotic expansion. The curve labeled "2-term" is computed from the first two terms of the expansion, and so on.

Rule (1) is illustrated by a comparison of the 1-term and 2-term partial sums with the exact result. In the range $ka \gtrsim 4$, the magnitude of the second term of the expansion is clearly small compared to the first term; the 2-term sum is very close to the 1-term sum, and both are quite accurate.

Rule (2) is illustrated by the behavior of the 1- and 2-term partial sums as $ka \to 0$. As ka decreases from 4, the magnitude of the ratio of the second-order term to the first-order term grows from 0.37 at $ka=4$ to 0.5 at $ka=3$, and then to 1 at $ka=1.5$, and finally approaches infinity as $ka \to 0$. At the same time, the accuracy of the first term diminishes. Nevertheless, for small ka, the best possible answer is still given by the leading-order term alone. Turning our attention back to Eq. 20, we see that for ρ fixed, as $k \to 0$, the correction term actually diverges, while the leading-order term vanishes. Judging from Senior's example, we expect it would be best to ignore the correction term entirely at "low" frequencies, where the threshold of the low-frequency regime could be defined as that frequency below which the correction term is about the same magnitude as or greater than the leading-order term.

With reference to rule (3), note that the figure indicates that for $ka \gtrsim 2$, the 3-term sum is a markedly better approximation than any of the other partial sums, thus showing how much the accuracy of the leading term of an asymptotic expansion can be improved upon by the proper use of higher-order terms. On the other hand for $ka \lesssim 1$, the 3-term sum yields a much worse approximation than either the 2- or 1-term sum. In many asymptotic series, the addition of just the lowest-order correction term alone to the leading-order term suffices to improve the accuracy over a range of the parameters involved. However, for Eq. 20 as for many asymptotic expansions encountered in practice, it is extremely difficult to determine *a priori* the optimum number of terms to use for maximum accuracy. One possible approach is to use as many terms as needed to give the best possible agreement with experiment.

F. Three Examples

Three examples are considered for which the integral of Eq. 5 can be evaluated analytically. Some observations on the theory's domain of validity are discussed.

1. Homogeneous Medium

For a homogeneous medium

$$c(z)=c(0)$$

and hence

$$n(z)=1.$$

While for such a medium there will be no turning points or caustics, it is of interest to compare the results of the asymptotic theory with the exact solution. We only have to consider the incident wave, for which

$$W(\xi,r,z)=\xi r+|z|(1-\xi^2)^{\frac{1}{2}},$$

$$W'(\xi,r,z)=r-|z|\xi(1-\xi^2)^{-\frac{1}{2}},$$

$$W''(\xi,z)=-|z|(1-\xi^2)^{-\frac{3}{2}}.$$

The equation $W'=0$ has only one root

$$\xi_1(1-\xi_1^2)^{-\frac{1}{2}}=r/|z|$$

or

$$\theta_1=\tan^{-1}(r/|z|),$$

which follows from the relation $\theta_j=\sin^{-1}\xi_j$.

Excluding the case $z=0$, corresponding to the horizontal ray $\theta_1=\pi/2$, we find that $W_1''<0$ for all z; hence there are no caustics. Substituting in Eq. 11, we obtain

$$\begin{aligned}p(r,z)&=\frac{P}{4\pi}\left[\frac{\xi_1}{r(1-\xi_1^2)W_1''}\right]^{\frac{1}{2}}e^{-ikW_1+i\pi/2}\\&=\frac{P}{4\pi}[\sin\theta_1\cos\theta_1/r|z|]^{\frac{1}{2}}\exp[ik(r\sin\theta_1+|z|\cos\theta_1)]\\&=(P/4\pi)(e^{ikR}/R),\end{aligned}$$

where

$$R=(r^2+z^2)^{\frac{1}{2}}.$$

Hence, in the absence of refraction, the asymptotic solution is identical to the exact solution.

Note that despite the use of the large argument approximation for $H_0^{(1)}(k\xi r)$ as an intermediate step in obtaining the asymptotic solution, the final result is valid for all frequencies and any distance from the source. Also, it can be verified that the lowest-order correction to the above result (which should be of order $1/k$) is identically zero. This suggests that all higher-order corrections may vanish as well, although this has not been proven.

2. *Medium with a Constant Velocity Gradient*

A medium with a sound velocity that increases linearly with depth,

$$c(z)=c_0(1-az),\quad a>0,$$
$$n(z)=1/(1-az),$$

gives rise to refraction phenomena and turning points. An exact solution for this case was obtained by Pekeris[27]:

$$p(r,z)=(P/2\pi a)[(1-az)^{\frac{1}{2}}/RR']\exp[i2\nu\tanh^{-1}(R/R')],$$

where

$$R=(r^2+z^2)^{\frac{1}{2}},$$
$$R'=[r^2+(z-2/a)^2]^{\frac{1}{2}},$$

and

$$\nu=(k^2/a^2-\tfrac{1}{4})^{\frac{1}{2}}.$$

We now obtain the ray solution. For a ray with $\xi<1$, the turning point is given by

$$z_\tau=(1/a)(1-1/\xi).$$

Hence

$$\varphi(z,\xi)=-\frac{1}{a}\left([1-\xi^2(1-az)^2]^{\frac{1}{2}}+\ln\left\{\frac{1-[1-\xi^2(1-az)^2]^{\frac{1}{2}}}{\xi(1-az)}\right\}\right),$$

$$\varphi'(z,\xi)=-[1-\xi^2(1-az)^2]^{\frac{1}{2}}/a\xi,$$

and

$$\varphi''(z,\xi)=\{a\xi^2[1-\xi^2(1-az)^2]^{\frac{1}{2}}\}^{-1}.$$

The ray solution is found by substitution in Eqs. 11 and 12. The result is

$$p(r,z)=\frac{P}{2\pi a}\frac{(1-az)^{\frac{1}{2}}}{RR'}\exp\left[i2\frac{k}{a}\tanh^{-1}\left(\frac{R}{R'}\right)\right].$$

This solution illustrates the behavior at the turning point described in Sec. I-C. As $z\rightarrow z_\tau$, $(n^2-\xi^2)^{\frac{1}{2}}=[1/(1-az)^2-\xi^2]^{\frac{1}{2}}\rightarrow 0$, but $\varphi''\rightarrow\infty$ as $[1/(1-az)^2-\xi^2]^{-\frac{1}{2}}$, and consequently there is no singularity in the denominator of Eqs. 11 or 12 at the turning point. Similarly, as $z\rightarrow z_\tau$, $\varphi(z)$ and $\varphi'(z)\rightarrow 0$, and the phases in Eqs. 11 and 12 become identical at the turning point, where we recall that in Eq. 11, $W''<0$ and the $\pi/2$ in the phase is canceled by an i in the denominator, which appears when the square root of W'' is taken. Hence, there is no abrupt phase shift at the turning point and furthermore, the ray solutions have well-defined identical limits at the turning point. This result agrees with the exact solution that displays no discontinuous or singular behavior at the turning points. We also note that for the turning-point reflected ray

$$W''(z,\xi)=[a\xi^2(1-\xi^2)^{\frac{1}{2}}]^{-1}+\{a\xi^2[1-\xi^2(1-az)^2]^{\frac{1}{2}}\}^{-1}>0\text{ for all }z;$$

hence no caustics are formed.

The relationship between the exact and ray solutions can be clarified further. By expanding ν into a series,

$$\begin{aligned}\nu&=(k^2/a^2-\tfrac{1}{4})^{\frac{1}{2}}\\&=\frac{k}{a}\left[1-\frac{1}{4(k/a)^2}\right]^{\frac{1}{2}}\\&=\frac{k}{a}\left[1-\frac{1}{2[4(k/a)^2]}-\frac{1}{8[16(k/a)^4]}-\frac{1}{16[64(k/a)^6]}-\cdots\right],\end{aligned}$$

we may write

$$\exp\left[i2\nu\tanh^{-1}\left(\frac{R}{R'}\right)\right]=\exp\left(i2\tanh^{-1}\left(\frac{R}{R'}\right)\times\left\{\frac{k}{a}-\frac{1}{2[4(k/a)]}-\frac{1}{8[16(k/a)^3]}-\frac{1}{16[64(k/a)^5]}-\cdots\right\}\right),$$

with which the exact solution can be transformed through use of the Taylor series expansion for the exponential to take the form

$$p(r,z)=\frac{P}{2\pi a}\frac{(1-az)^{\frac{1}{2}}}{RR'}\exp\left[i2\nu\tanh^{-1}\left(\frac{R}{R'}\right)\right]$$

$$=\frac{P(1-az)^{\frac{1}{2}}}{2\pi aRR'}\exp\left[i2\frac{k}{a}\tanh^{-1}\left(\frac{R}{R'}\right)\right]$$

$$\times\left[1-\frac{[i2\tanh^{-1}(R/R')]}{2[4(k/a)]}-\frac{[i2\tanh^{-1}(R/R')]^2}{2\{4[16(k/a)^2]\}}\right.$$

$$\left.-\frac{[i2\tanh^{-1}(R/R')]}{8[16(k/a)^3]}+\cdots\right].$$

The first term in the expansion of the exact solution is seen to be the ray-acoustics solution. The ray-acoustics solution is therefore an accurate approximation when the higher-order terms in the expansion are small. For a fixed location (R, R' fixed), the higher-order terms will vanish as $k/a\rightarrow\infty$. Hence the ray solution is accurate when $\omega\gg\partial c/\partial z$, i.e., when the frequency is much larger than the gradient of the velocity profile.

For k/a fixed, we examine the behavior of the quantity $\tanh^{-1}(R/R')$ as a function of location to determine how the accuracy of the ray solution depends on position. Since $\tanh^{-1}x$ is a function that increases monotonically from zero at $x=0$ to infinity as $x\rightarrow 1$, $\tanh^{-1}(R/R')\rightarrow 0$ as $R\rightarrow 0$ while $\tanh^{-1}(R/R')\rightarrow\infty$ as $R\rightarrow\infty$ [since $(R/R')\rightarrow 1$ as $R\rightarrow\infty$]. Hence, for any given value of k/a, the ray solution's accuracy decreases with increasing range from the source.

Our results can be interpreted as follows. When the propagating wave is sufficiently close to the source, the medium's effect must be small and the wave must look very much like that from a point source in a homogeneous medium. We would therefore expect from the previous example that our theory should give an accurate result in the source vicinity. We see from the exact solution that the correction terms to the ray solution will indeed be small close in, and it can be verified that the ray-acoustics solution approaches the limit $Pe^{ikR}/4\pi R$ as $R\rightarrow 0$. As the wave moves away from the source, the influence of the medium becomes progressively more important, and the effects of refraction cause the ray-acoustics solution to alter from its close-in behavior and the correction terms to grow in importance.

This result supports the observation we made in the first example about the use of the large argument expansion of $H_0^{(1)}(k\xi r)$ in obtaining the ray-acoustics solution. We conclude that the accuracy of ray acoustics does not necessarily depend on the condition $kr\gg 1$.

We should also note that the higher-order corrections to the ray solution, as well as the ray solution itself, show no unusual behavior at the turning points of the rays. Thus, although the WKB approximation is used as an intermediate step in obtaining the ray-acoustics result, and although it is well known that the WKB method breaks down in the vicinity of the turning points of Eq. 2, the accuracy of the ray-acoustics solution does not deteriorate as the field point approaches the ray turning points. The explanation of this apparent paradox is that if Eq. 2 is thought of as describing one-dimensional wave propagation, the turning point of Eq. 2 corresponds to a caustic and the WKB solution will indeed diverge there. However, we are in reality considering two-dimensional wave propagation, for which it is well known that the ray-acoustics solution and the higher-order corrections to it are well behaved at ray turning points. The ray solution diverges only at a caustic which, in the two-dimensional case, is always separated from the turning points of the rays.

3. *Medium with a Bilinear Profile*

A medium with a bilinear sound-speed profile will display the formation of a caustic. We assume the sound speed defined by

$$c(z)=c_0,\qquad z>0,$$
$$c(z)=c_0(1-az),\quad z<0.$$

While this profile is very similar to one considered by Brekhovskikh[28] and identical to that studied by Friedman,[29] it happens to be an appropriate model for the experiment analyzed in this paper and, in addition, it provides another illustration of the application of the general formulation we have developed to a specific profile.

We assume the source to be at a height z_0 above the origin rather than at the origin itself. We obtain the turning-point-reflected ray solution for $z>0$ only.

The ray solution for the wave reflected at the turning point is given by

$$p(r,z)=\frac{P}{4\pi}\sum_j\left[\frac{\xi_j}{r(1-\xi_j^2)W_j''}\right]^{\frac{1}{2}}e^{ikW_j},$$

where

$$W(\xi,r,z)=\xi r+\varphi(z)+\varphi(z_0)$$
$$=\xi r+(z+z_0)(1-\xi^2)^{\frac{1}{2}}-2a^{-1}\times[(1-\xi^2)^{\frac{1}{2}}-\tanh^{-1}(1-\xi^2)^{\frac{1}{2}}],$$
$$W'=r-(z+z_0)\xi(1-\xi^2)^{-\frac{1}{2}}-2(a\xi)^{-1}(1-\xi^2)^{\frac{1}{2}},$$
$$W''=-(z+z_0)(1-\xi^2)^{-\frac{3}{2}}+2(a\xi^2)^{-1}(1-\xi^2)^{-\frac{1}{2}}.$$

Letting $W'=0$, we obtain a quadratic equation in the variable $\xi(1-\xi^2)^{-\frac{1}{2}}$. For $r=r_c\equiv[8a^{-1}(z+z_0)]^{\frac{1}{2}}$, we find that $W''=0$ as well, and that the quadratic equation has one real root

$$\xi_c=[4(z+z_0)^2+r_c^2]^{-\frac{1}{2}}r_c,$$

corresponding to the caustic.

For $r>r_c$, there are two real roots given by

$$\xi_{\substack{1\\2}}(1-\xi_{\substack{1\\2}}^2)^{-\frac{1}{2}}=\frac{r}{2(z+z_0)}\pm\left[\frac{r^2}{4(z+z_0)^2}-\frac{2}{a(z+z_0)}\right]^{\frac{1}{2}},$$

corresponding to the rays approaching and receding from the caustic; and for $r<r_c$, no real roots exist, corresponding to the shadow zone.

Figure 6 shows the ray diagram corresponding to this model. The caustic has two branches, only one of which penetrates into the region $z>0$. Note that each ray has passed through a turning point before it encounters the caustic and also that the rays have only one point of tangency with a caustic.

The two branches meet at a cusp. At the cusp, $W'''=0$ and hence the caustic boundary-layer solution breaks down. For a treatment of this region, see Brekhovskikh.[30]

We can get some further insight into the accuracy of the caustic boundary-layer solution by evaluating the magnitude of the ratio of the correction term to the caustic boundary-layer solution. Confining our attention to the caustic itself, after substitution of the formulas for ξ_c and r_c into Eq. 20, this ratio becomes

$$\left(\frac{1}{2}\right)^{\frac{1}{3}}\left|\frac{\mathrm{Ai}'(0)}{\mathrm{Ai}(0)}\right|\frac{1}{|k/a|^{\frac{1}{3}}}\frac{[a(z+z_0)/2]^{\frac{1}{2}}}{[1+a(z+z_0)/2]^{\frac{1}{2}}}.$$

From the discussion in Sec. I-E, it will be recalled that the caustic boundary-layer solution is expected to be accurate when this ratio is small compared to unity.

For a fixed location (z fixed), the ratio goes to zero as $|k/a|^{\frac{1}{3}}$ goes to infinity. That is, the caustic boundary-layer solution will be accurate for frequencies much larger than the velocity gradient in the region $z<0$. If we prefer, we can think of k as fixed and a as a variable. Since the medium becomes homogeneous everywhere in the limit $a\rightarrow 0$, the magnitude of a is a measure of the amount of refraction present. Now the ratio increases as a increases; hence we conclude that the larger the velocity gradients and the more pronounced the refraction, the larger the error in the caustic boundary-layer solution.

For fixed $|k/a|$, the ratio increases monotonically with increasing z. From the ray diagram of Fig. 6, it will be noted that the separation between a given point on the caustic and the turning point of the ray through that same point on the caustic increases with increasing height. This suggests that the accuracy of the caustic boundary-layer solution diminishes with increasing distance between the caustic point and the turning point of the related ray.

II. REFRACTION AND FOCUSING FROM A TRANSIENT SOURCE

The ray-acoustics and caustic boundary-layer solutions developed in Sec. I for a harmonic source are used

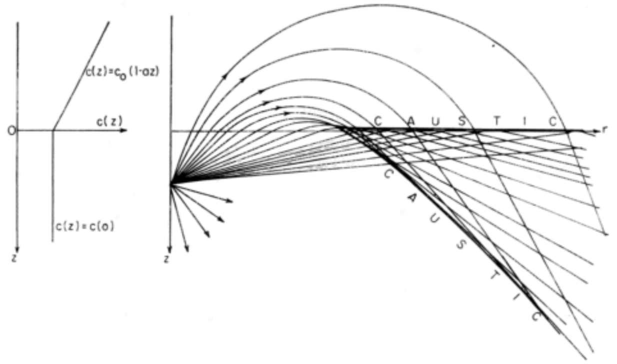

FIG. 6. Bilinear sound-speed profile and associated ray diagram.

to describe transient sources by means of Fourier transformation. The properties of the transient forms of the ray-acoustics solutions are studied, and it is shown that the ray solution that has passed through a caustic exhibits a precursor and an infinite peak pressure for steep-fronted source pulses. The transient form of the caustic boundary-layer solution is likewise found to distort the initial source pulse severely, constricting its width, adding a precursor, and yielding an infinite peak pressure for source pulses with abrupt steps. The use of the correction terms to the caustic boundary-layer solution in the time-dependent case is discussed. Finally, the inclusion of viscous effects into the theory is described.

A. Fourier Transformation of the Harmonic Solutions

The solution for a transient source can be obtained from the solution for a harmonic source by Fourier transformation. We again start with an initially spherical wave near the origin of the form

$$p(R,t)=\frac{F(t-R/c)}{4\pi R}. \tag{21}$$

The governing time-dependent wave equation is given by

$$\nabla^2 p-[1/c^2(z)]\,(\partial^2/\partial t^2)p=-\delta(x)\delta(y)\delta(z)F(t).$$

The Fourier transform

$$\tilde{p}(\omega)=\int_{-\infty}^{+\infty}p(t)e^{i\omega t}dt$$

satisfies the transformed equation

$$\nabla^2\tilde{p}+k^2n^2(z)\tilde{p}=-\tilde{F}(\omega)\delta(x)\delta(y)\delta(z),$$

which is identical to the equation for the harmonic source, provided we replace the amplitude factor P by the transform of the transient pulse, $\tilde{F}(\omega)$. The time-dependent solution is given by the inverse transform of the harmonic solution

$$p(r,z,t)=\frac{1}{2\pi}\int_{-\infty}^{+\infty}e^{-i\omega t}\tilde{p}(r,z,\omega)d\omega. \tag{22}$$

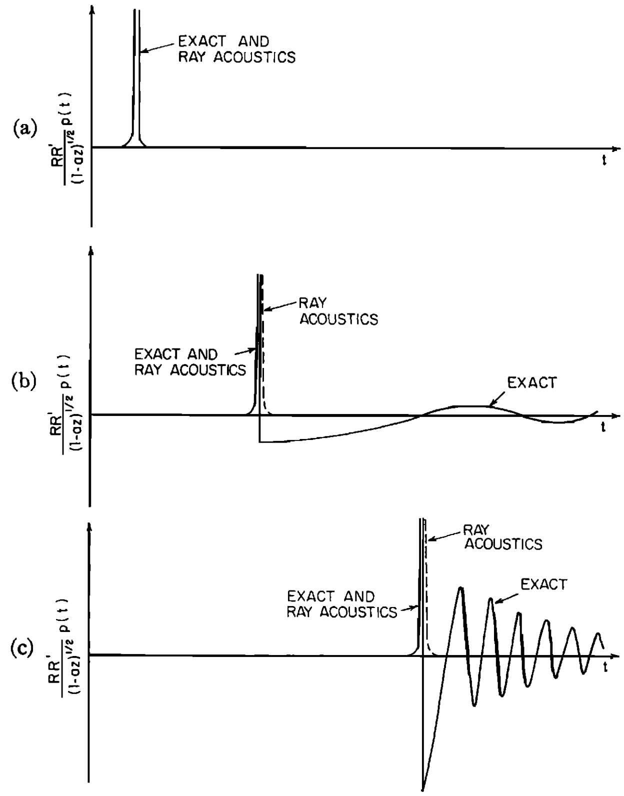

FIG. 7. Comparison of exact and ray-acoustics pressure–time histories for an impulsive point source in a constant-velocity-gradient medium. (a) $R\approx 0$; (b) $R=R_1\neq 0$; (c) $R=R_2\gg R_1$.

The range of integration includes negative as well as positive frequencies. In Sec. I, we have tacitly assumed ω to be positive. Extension to negative frequencies is accomplished by imposing the physical requirement that $p(r,z,t)$ be real for all t. This implies that

$$\tilde{p}(r,z,-\omega)=\tilde{p}^*(r,z,\omega), \tag{23}$$

where the asterisk denotes complex conjugate. Hence, if our solutions are to be extended to negative frequencies, they must be modified by means of Eq. 23.

B. The Ray Solution

In instances where a caustic has not been encountered by a ray, it has been shown that $W''<0$ for a wave that has not passed through a turning point, while $W''>0$ for one that has. From Eqs. 11 and 12, both cases can be represented by the formula

$$\tilde{p}(r,z,\omega)=\frac{\tilde{F}(\omega)}{4\pi}\left[\frac{\xi}{r(1-\xi^2)^{\frac{1}{2}}(n^2-\xi^2)^{\frac{1}{2}}|W''|}\right]^{\frac{1}{2}}e^{ikW(r,z)},$$

where ξ is a solution of $W'=0$. Note that this expression automatically satisfies Eq. 23. From Eq. 22 we obtain

$$p(r,z,t)=\frac{F[t-W(r,z)/c]}{4\pi}\left[\frac{\xi}{r(1-\xi^2)^{\frac{1}{2}}(n^2-\xi^2)^{\frac{1}{2}}|W''|}\right]^{\frac{1}{2}}. \tag{24}$$

The time history of the pulse apparently undergoes no distortion, and the delay given by W/c equals the travel time of the pulse along the ray. This result is not, in general, rigorously valid because it is based on a high-frequency approximation. Since the front of a pulse of any arbitrary shape is determined by the high-frequency portion of the spectrum, we expect Eq. 24 to yield a good description of the pulse onset. It will not, in general, give valid results at large times beyond the passing of the front.

The accuracy of Eq. 24 also depends upon the nonhomogeneity of the medium. For example, in a homogeneous medium, the ray solution, Eq. 24, is exact for all times. For a medium with a constant velocity gradient, it can be seen from our discussion in Sec. I-F that the ray solution is a good approximation over a large time range for observation points close to the source, but that as the distance to the source increases, the accuracy of the ray theory in the time domain beyond the front decreases. This type of behavior can be verified using the results of Myers,[31] who gives an exact solution for a δ-function pulse (see Fig. 7). Close to the source, the exact pressure time history is a δ function, the same as ray acoustics would predict [Fig. 7(a)]. As the pulse propagates, it develops a tail behind the front [Fig. 7(b)], which becomes progressively more pronounced as the range increases [Fig. 7(c)]. These two examples suggest that if refractive effects are absent (as in the first example) or if they have not had a chance to take effect (as in the case of the nearby observation point in the second example), then the ray solutions will be accurate over a long time domain. But as the pulse propagates, the effects of refraction accumulate, and the ray solution becomes less and less accurate for epochs beyond the wavefront.

For a ray which has passed through a caustic, the term W'' in the denominator of the ray solution will become negative, contributing a $\pi/2$ term to the phase:

$$\tilde{p}(r,z,\omega)=\frac{\tilde{F}(\omega)}{4\pi}\left[\frac{\xi}{r(1-\xi^2)^{\frac{1}{2}}(n^2-\xi^2)^{\frac{1}{2}}|W''|}\right]^{\frac{1}{2}}\times\exp[ikW(r,z)-(i\pi/2)\mathrm{sgn}\omega],$$

where the function

$$\mathrm{sgn}\omega=|\omega|/\omega$$

multiplies the phase shift in order to comply with Eq. 23. While the phase shift appears to be of little consequence for harmonic waves, it leads to significant distortion for transient pulses. For example, a transient pulse, upon undergoing a $\pi/2$ phase shift in the frequency domain, is changed into a Hilbert transform in the time domain[32]

$$p(r,z,t)=\frac{1}{4\pi}\left[\frac{\xi}{r(1-\xi^2)^{\frac{1}{2}}(n^2-\xi^2)^{\frac{1}{2}}|W''|}\right]^{\frac{1}{2}}F_H\left[t-\frac{W(r,z)}{c}\right], \tag{25}$$

where

$$F_H(t)=\frac{1}{\pi}\,\mathrm{Pr}\int_{-\infty}^{\infty}\frac{F(\tau)}{\tau-t}d\tau,$$

and Pr denotes principal value.

Figure 8 shows some pulses together with their Hilbert transforms. The transformed pulses have two characteristics that are unacceptable on physical grounds:

(1) precursors extending back to $t\rightarrow\rightarrow\infty$;

(2) logarithmic singularities corresponding to step discontinuities in the pulse.

We discuss the implications of these features on the validity of the theory. They are associated with, respectively, the lower and upper limits of the frequency spectrum.

1. *Precursors*

Since the solution in the frequency domain was based on a high-frequency approximation, it is not necessarily correct in the low-frequency limit. Unreasonable behavior at large times, whether positive or negative, is therefore understandable in terms of the approximations used.

2. *Singularities*

The singularities in the transformed pulse are not the consequence of any approximations made within the theory. While, strictly speaking, step discontinuities are physically unrealizable because of the presence of dissipative processes, the theory will predict exceedingly large amplitudes for explosive pulses, which have very short risetimes, so that the validity of the linear acoustic approximation for predicting the peak pressure is brought into question.

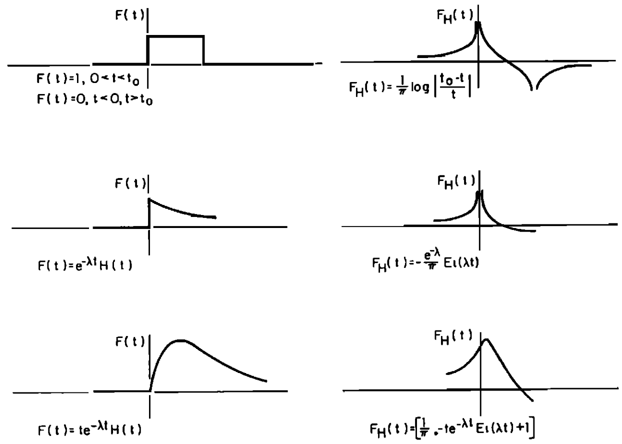

FIG. 8. Three simple pulse shapes and their Hilbert transforms.

C. The Transient Field at a Caustic

In the vicinity of the caustic, we obtain using Eq. 14

$$p(r,z_c,t)=\frac{1}{8\pi^2}\int_{-\infty}^{\infty}\tilde{F}(\omega)\,|k|^{1/6}\zeta\times\left[\frac{2\pi\xi_c}{r(n^2-\xi_c^2)^{\frac{1}{2}}(1-\xi_c^2)^{\frac{1}{2}}}\right]^{\frac{1}{2}}\mathrm{Ai}(\pm|k|^{\frac{2}{3}}\zeta\Delta r)\times\exp\{i[kW_c-\omega t-(\pi/4)\,\mathrm{sgn}\omega]\}d\omega,\quad (W_c'''\gtrless 0). \tag{26}$$

Because the caustic field solution initially increases with frequency as $|\omega|^{1/6}$, the amplification due to focusing will be most pronounced for the high-frequency components. The discussion of Sec. II-B suggests that because of the presence of the term $(\pi/4)\mathrm{sgn}\omega$ in the phase, the pulse shape will change radically as we approach the caustic. On the caustic, near where the highest intensities occur, we can obtain the time history from Eq. 26 with $\Delta r=0$, or

$$p(r,z_c,t)=\frac{1}{8\pi^2}\left[\frac{2\pi c^{-\frac{1}{3}}\xi_c}{r(n^2-\xi_c^2)^{\frac{1}{2}}(1-\xi_c^2)^{\frac{1}{2}}}\right]^{\frac{1}{2}}\zeta\,\mathrm{Ai}(0)\times\int_{-\infty}^{+\infty}\tilde{F}(\omega)\,|\omega|^{1/6}\exp\{i\omega[W_c/c-t-(\pi/4)\,|\omega|\,]\}d\omega.$$

Figure 9 shows the time history of the pressure pulse on the caustic for a triangular pulse. The time history exhibits drastic distortion and an infinitely long precursor. In addition, the peak pressure will become infinite if the risetime of the initial pulse vanishes. In this instance, the pressure–time history can be shown to have a term whose time dependence is proportional to $|t-W_c/c|^{-1/6}$.

The "corrected" caustic boundary-layer solution of Eq. 20 can be used to calculate a time history that may be somewhat more accurate than the result of Eq. 26. Recalling the restriction of Eq. 15 and also the discussion following Eq. 20, and using Eq. 20, we obtain

$$p(r,z_c,t)=\frac{1}{8\pi^2}\int_{-\infty}^{+\infty}\tilde{F}(\omega)\,|k|^{1/6}\zeta\left[\frac{2\pi\xi_c}{r(n^2-\xi_c^2)^{\frac{1}{2}}(1-\xi_c^2)^{\frac{1}{2}}}\right]^{\frac{1}{2}}\mathrm{Ai}(\pm|k|^{\frac{2}{3}}\zeta\Delta r)\exp\left[i\left(kW_c-\omega t-\frac{\pi}{4}\,\mathrm{sgn}\omega\right)\right]d\omega+\frac{1}{8\pi^2}$$
$$\times\left[\int_{-\omega_{\max}}^{-\omega_{\min}}+\int_{\omega_{\min}}^{\omega_{\max}}\right]\frac{\tilde{F}(\omega)}{|k|^{1/6}}\left\{\mp\zeta^2\frac{\partial}{\partial\xi}\left[\frac{2\pi\xi}{r(n^2-\xi^2)^{\frac{1}{2}}(1-\xi^2)^{\frac{1}{2}}}\right]^{\frac{1}{2}}\Bigg|_{\xi=\xi_c}\mathrm{Ai}'(\pm|k|^{\frac{2}{3}}\zeta\Delta r)+\frac{\zeta^5}{24}\left[\frac{2\pi\xi_c}{r(n^2-\xi_c^2)^{\frac{1}{2}}(1-\xi_c^2)^{\frac{1}{2}}}\right]^{\frac{1}{2}}W_c''''\right.$$
$$\left.\times\left[2\,\mathrm{Ai}'(\pm|k|^{\frac{2}{3}}\zeta\Delta r)+|k|^{\frac{2}{3}}\zeta^2(\Delta r)^2\,\mathrm{Ai}(\pm|k|^{\frac{2}{3}}\zeta\Delta r)\right]\right\}\exp\left\{i\left[kW_c-\omega t+(\pi/4)\,\mathrm{sgn}\omega\right]\right\}d\omega,\quad (W_c'''\gtrless 0). \tag{26'}$$

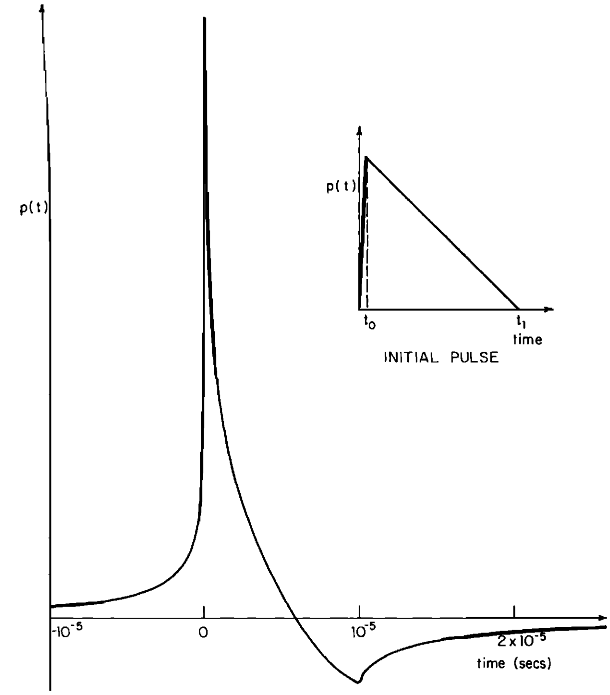

FIG. 9. Transient waveform at a caustic for a triangular pulse. The risetime t_0 of the pulse is 10^{-7} sec and the duration t_1 is 10^{-5} sec.

Here $\omega_{\mathrm{max}}\approx c/(\zeta|\Delta r|)^{\frac{3}{2}}$, which follows from Eq. 15, and ω_{min} is the frequency at which the correction term is about the same magnitude as the caustic boundary-layer solution. The choice of ω_{min}, it will be recalled, follows from the discussion of Senior's results given in Sec. I-E.

D. Viscous Effects

We have seen that the peak pressure of a steep-fronted pulse will become infinite at a caustic and remain so over its subsequent propagation path. However, a propagating medium of practical interest, such as the ocean, exhibits viscous damping. The incorporation of viscosity into the theory ensures finite pressure levels.

An approximate treatment of viscous effects is now given. Close to the source, the pressure is an initially spherical wave as in Eq. 21. The time-dependent wave equation, including viscous damping terms, is[33]

$$\nabla^2 p-\frac{1}{c^2(z)}\frac{\partial^2}{\partial t^2}p+\frac{\nu}{c^2(z)}\frac{\partial}{\partial t}\nabla^2 p =-\delta(x)\delta(y)\delta(z)\left[F(t)+\frac{\nu}{c^2(0)}\frac{\partial}{\partial t}F(t)\right],$$

where ν is the kinematic viscosity coefficient

$$\nu=(\eta+\tfrac{4}{3}\mu)/\rho,$$

where η is the coefficient of bulk viscosity, μ the coefficient of shear viscosity, and ρ the density of the medium.

For a sinusoidal source ($e^{-i\omega t}$ time dependence) of strength $\tilde{F}$, the viscous wave equation becomes

$$\nabla^2\tilde{p}+\frac{k^2n^2(z)}{[1-i\omega\nu/c^2(z)]}\tilde{p}=-\delta(x)\delta(y)\delta(z)\tilde{F}.$$

If $|\omega\nu/c^2(z)|\ll 1$ and the variation of $c(z)$ in the spatial domain of interest is small enough, then in the factor $[1-i\omega\nu/c^2(z)]$, $c(z)$ may be replaced by $c(0)$ and an effective propagation constant may be defined:

$$k_v\equiv\frac{k}{[1-i\omega\nu/c^2(0)]^{\frac{1}{2}}} \cong k\left[1+\frac{ik\nu}{2c(0)}\right]. \tag{27}$$

In situations of practical interest, these approximations will be valid up to very high frequencies. For example, in fresh water, $\omega\nu/c^2$ is about 0.1 for a frequency of 10^{10} Hz. For the steady-state wave equation we obtain

$$\nabla^2\tilde{p}+k_v^2n^2(z)\tilde{p}=-\delta(x)\delta(y)\delta(z)\tilde{F},$$

corresponding to Eq. 1. The development of the ray solutions and caustic field solution now evolves as in the inviscid case, the only difference being the appearance of k_v instead of k. In the first approximation, using Eq. 27, the transient field in the caustic vicinity is given by

$$p(r,z_c,t)=\frac{\zeta}{8\pi^2}\left[\frac{2\pi\xi_c{}^2c^{-\frac{1}{3}}}{r[n^2(z_c)-\xi_c{}^2]^{\frac{1}{2}}(1-\xi_c{}^2)^{\frac{1}{2}}}\right]^{\frac{1}{2}} \times\int_{-\infty}^{+\infty}\tilde{F}(\omega)|\omega|^{1/6}\,\mathrm{Ai}(\pm|k|^{\frac{2}{3}}\zeta\Delta r) \times\exp\left\{-i\omega\left[t-\frac{W_c(r)}{c}\right]-\frac{\nu W_c(r)}{2c^3}\omega^2-\frac{i\pi}{4}\mathrm{sgn}\omega\right\}d\omega. \tag{28}$$

The absorption factor $\exp\{-\nu W\omega^2/2c^3\}$, which appears in the caustic boundary-layer solution (and which will also appear in the ray solution) will guarantee finite peak pressures, even for pulses with vanishing risetimes near the source. The net effect of viscosity is to cause the pulse to acquire a nonzero risetime by the time it reaches the caustic.

III. COMPARISON OF THEORY AND EXPERIMENT

In their experiment, Barash and Goertner[1] detonated a small ($\frac{1}{8}$-lb) submerged pentolite explosive charge in a body of water with a depth-dependent sound-speed profile as shown to the left of Fig. 10. To the right is the associated ray diagram. A group of the rays emanating from the source intersect in such a way that an envelope, the caustic, is formed. With a vertical array of hydrophones, Barash and Goertner observed the pressure pulses produced at points in the vicinity of the caustic at a horizontal range of 300 ft from the charge (see Fig. 11).

The theory requires two items as input data before predictions can be made: a sound-speed profile and a specification of the pressure pulse at the sound source, the pentolite charge in this case. We discuss each item separately.

A. Model Sound-Speed Profile

Since it appears to be a reasonable fit to the data, we use a bilinear profile as shown in the left half of Fig. 6. The associated ray diagram exhibits a two-branched caustic. The almost horizontal branch corresponds to the experimental caustic. The lower branch of the theoretical caustic is superfluous to the analysis of the experiment. It appears only because the surface isovelocity layer of the actual profile has been omitted from our model; had it been included, the superfluous branch would extend down from the cusp only a short distance. This can be understood by observing that all rays emitted at too large an angle with respect to the $+z$ axis would not pass through a turning point before encountering the isovelocity layer. Their subsequent paths—straight lines followed by reflection at the water surface—would not permit formation of the lower caustic branch beyond a certain range.

However, the "lateral wave," a signal with a distinct onset which is sometimes observed to occur prior to the caustic-related pulse, probably owes its origin to the existence of the surface layer. The small amplitude signals preceding the large peaks in the experimental records of Fig. 11 may be lateral waves. Normally, lateral waves are thought of as disturbances that travel along an interface at which the speed of sound undergoes an abrupt change and that radiate energy into the region of lower sound speed.[34] However, it has been theoretically demonstrated[35] that lateral wave-type propagation can occur in the case of two isovelocity half-spaces whose sound speeds differ and which are connected by an arbitrary transition layer. The lateral wave will propagate along the intersection between the transition region and the half-space with

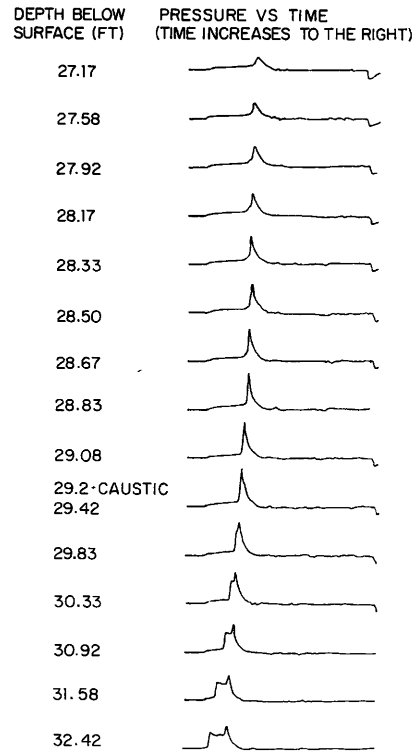

FIG. 11. Pressure pulses observed near caustic (from Barash and Goertner, Ref. 1).

the higher sound speed. In the experiment we are considering, it seems likely that lateral waves could be excited along the intersection of the surface isovelocity layer and the transition region extending from about 15 ft to about 30 ft in depth. The ray diagram in Fig. 10 shows rays traveling almost horizontally at a depth of about 15 ft, and these may, in fact, correspond to lateral waves. Since the model we have selected does not have an upper isovelocity regime, it will be unable to predict this type of signal.

The omission of the water surface from the model profile is of no concern since a surface-reflected pulse arrives at the caustic much later than the caustic-focused pulse.

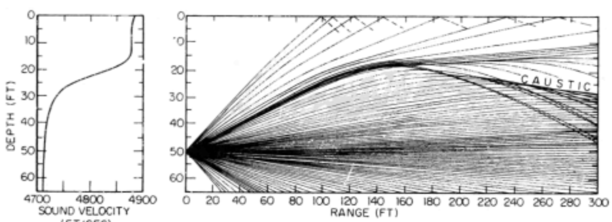

FIG. 10. Experimental sound-speed profile and associated ray diagram.

B. Model Explosive Pulse

The pressure pulse produced in the vicinity of a submerged explosive is generally described as having a negligible risetime and an exponential decay, the decay constant and peak pressure being functions of the charge weight, type, and the range. The pressure pulse for a pentolite charge is described empirically out to moderate distances by[16]

$$p(R,t)=2.25\times10^4(W^{\frac{1}{3}}/R)^{1.13}e^{-t/t_D}\quad(\text{in lb/in.}^2),$$

where p is the instantaneous pressure at time t after the onset of the shock front and t_D is the decay constant of the exponential pulse or the time for the pressure to

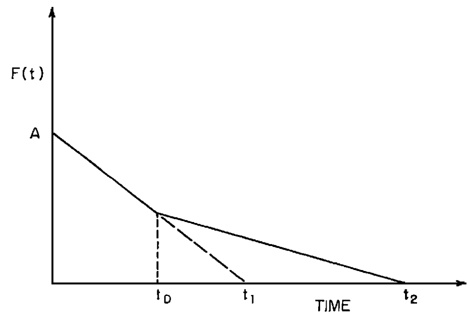

FIG. 12. Theoretical time history.

decay to $1/e=0.368$ of its initial value. The decay constant is given by

$$t_D = 58W^{\frac{1}{3}}\left(\frac{W^{\frac{1}{3}}}{R}\right)^{-0.22} \quad (\mu\text{sec}),$$

where W is the weight of the charge in pounds and R is the range from the source in feet.

Our theory, on the other hand, allows a pressure pulse of the form

$$p(R,t) = \frac{F(t-R/c)}{4\pi R}$$

in the vicinity of the source. The theory allows only spherical spreading, while the empirical expressions involve an inverse power of the range somewhat larger than unity. The discrepancy is a manifestation of the omission of finite-amplitude effects. As a result, the theoretical predictions depend upon the range at which the theoretical and empirical pressure pulses are made to coincide. For example, as the matching point is moved outward from 1 to 10 charge radii (the charge radius was 0.068 ft), the predicted peak amplitude on the caustic decreases by 30%. We chose the matching point at 10 charge radii.

For mathematical convenience, the theoretical time history is taken to be a continuous function composed

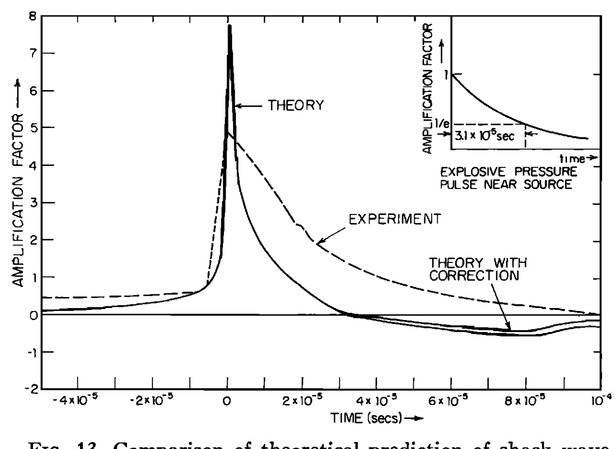

FIG. 13. Comparison of theoretical prediction of shock waveform at a caustic with experimental waveform.

of two straight line segments (Fig. 12),

$$\begin{aligned} F(t) &= 0, && t<0, \\ &= A(t_1-t)/t_1, && 0\le t\le t_D, \\ &= A\frac{(t_1-t_D)}{(t_2-t_D)}\frac{(t_2-t)}{t_1}, && t_D\le t\le t_2, \\ &= 0, && t>t_2, \end{aligned}$$

where t_D is the empirical decay time at 10 charge radii. The three free constants, A, t_1, and t_2, are determined by requiring that the model expression match the empirical pressure pulse in peak value (at $t=0$), at $t=t_D$ and at $t=2t_D$. As a consequence, the theory cannot yield valid predictions for times on the order of $2t_D$ or larger after peak value occurs. Since the theory is a high-frequency asymptotic theory, accuracy for large times cannot be expected in any case.

The theoretical prediction obtained using Eq. 28 is compared with experiment in Fig. 13. The ordinate is the amplification factor: the ratio of the theoretically predicted—or experimentally observed—pressure on the caustic to the peak pressure which would have been seen at the same point of observation if the medium were nonrefracting. In the upper right of the figure is the time history of the explosive pressure pulse near the source.

The theoretically predicted peak value is about 60% too large, while the remainder of the theoretical time history falls significantly below the experimental curve.

The curve labeled "Theory with Correction" shows the effect of using the correction term discussed in Sec. I-F. The correction term was added to the caustic boundary-layer solution and the resultant expression used to calculate the waveshape according to the prescription given in Eq. 26′. The minimum frequency of application of the correction term was chosen to be $\omega_{\min}=10^3$ (see Fig. 14), although a choice of a lower minimum frequency, even down to $\omega=1$, does not alter the final result in any important way. Figure 14 suggests that the asymptotic errors in the theory will begin to be noticeable for circular frequencies of about 10^3 or 10^4; in the time domain, we might expect the theoretically predicted time history to become inaccurate for times larger than about 10^{-4} sec. The "corrected" theoretical curve of Fig. 13 supports this conclusion; the time-dependent correction term is clearly insignificant over the time range shown. The influence of asymptotic errors in the theory on the accuracy of the predicted pulse shape is therefore unimportant, and the discrepancy between theory and experiment must be attributable to other factors. The most likely sources of error are (1) the neglect of finite amplitude effects; (2) the omission from the theory of the distorting effects of the experimental equipment; and (3) the absence of a lateral wave.

1. *Finite-Amplitude Effects*

Probably the most important deficiency of the theory is the assumption that the laws of linear acoustics are valid. Even for explosive pulses in isovelocity water where the complications of refraction are absent, the discrepancy between experiment and predictions of the present theory is quite pronounced (Fig. 15). Since linear acoustics neglects the complicated dissipative processes physically occurring as well as the dependence of the propagation speed on pressure amplitude, the theory predicts too large a peak pressure at any given range, while the decay constant is predicted to be independent of distance and to be smaller than the observed values. We might therefore anticipate that even in the presence of refractive effects, the incorporation of finite-amplitude effects into the present theory would tend to lower the predicted peak pressure in Fig. 13 and to increase the predicted decay time. Work on the incorporation of nonlinear effects into the present theory is currently in progress. A method of accounting for nonlinearities is described in the accompanying paper by Blatstein.[15]

2. *Hydrophone Response*

Another factor that may contribute to the overly large predicted peak pressure in Fig. 13 is the neglect, in the theoretical computations, of the high-frequency cutoff of the hydrophones used in the experiment. Inclusion of the hydrophone response would suppress the high-frequency components of the theoretical pulse and thereby lower the peak value. For example, the gauge response completely suppresses all frequencies above 3×10^5 Hz,[36] while at a frequency of 5×10^5 Hz, the fractional attenuation due to viscosity alone is about 0.6. Hence, the gauge cutoff overwhelms the effects of viscous attenuation. Blatstein,[15] in his analysis of experimental results similar to those considered here, includes the gauge response in his computations and finds that the theoretically predicted peak pressure agrees very closely with experiment.

3. *Lateral Wave*

Prior to the occurrence of the peak pressure, the theoretical and experimental time histories show a significant discrepancy. In this time regime (and perhaps later as well), the observed pressure may consist of a superposition of the tail of a lateral wave and the caustic-focused pulse. This could possibly account for the larger values of the observed pressures as compared to the theory, which does not include an isovelocity surface layer in the sound-speed profile and consequently will not predict a lateral wave. Work on the incorporation of a lateral wave into the theory is in progress, however, and the results will be reported at some future date.

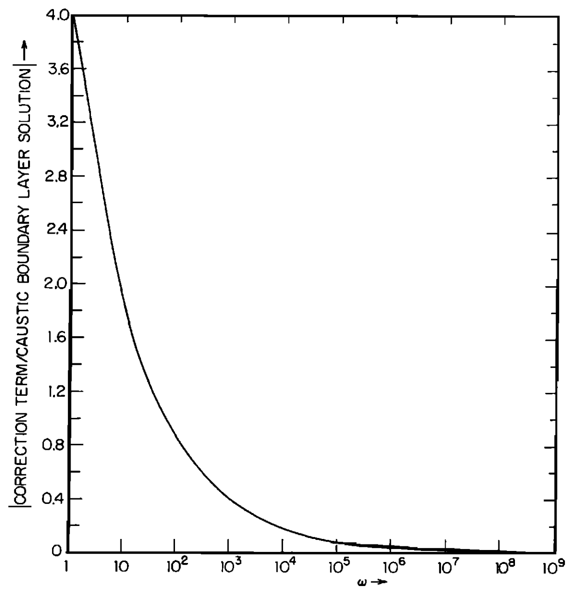

FIG. 14. Relative magnitude of the correction term and the caustic boundary-layer solution as a function of frequency.

IV. SUMMARY AND CONCLUSIONS

An asymptotic theory has been developed to describe the focusing and refraction of both harmonic sound and transient pulses emanating from a point source in an arbitrarily stratified medium. Away from focusing regions, the theory is equivalent to geometrical acoustics. In the vicinity of caustics, the theory predicts, for harmonic waves, a spatially oscillating field amplitude on the illuminated side of the caustic with the peak pressure near, but not quite on, the caustic. In the shadow zone, the field is damped with increasing distance from the caustic boundary. Transient pulses in the focusing zone will exhibit severe distortion, of which the most striking features are amplification of the peak pressure, narrowing of the pulse width, and a precursor. The influence of the approximate asymptotic methods employed in the theory on its domain of validity is discussed in some detail. A quantitative means of estimating the theory's accuracy in the vicinity of caustics is derived. Generally, it appears that the inaccuracies of the theory increase with increasing

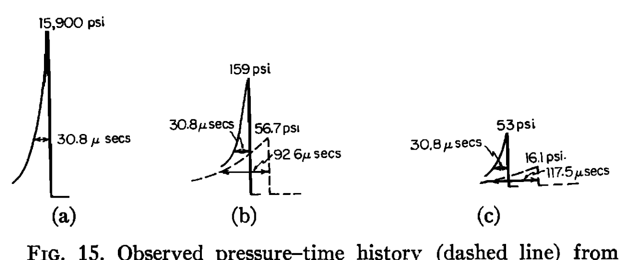

FIG. 15. Observed pressure–time history (dashed line) from $\frac{1}{8}$-lb Pentolite explosive source in nonrefracting medium compared with time history predicted by theory (solid line). R is the range from the source. For clarity of presentation, differences in arrival times are not drawn to scale. (a) $R=0.68$ ft; (b) $R=100$ ft; (c) $R=300$ ft.

sound-velocity gradients and/or increasing distance along a ray from the source.

A comparison of the theory with the results of an experiment involving underwater explosives shows that a reasonable prediction of the peak pressure at a caustic can be obtained. However, the predicted pulse-width is too narrow, most probably as a result of the neglect of nonlinear effects.

ACKNOWLEDGMENTS

This work was sponsored by the Field Projects Branch of the Office of Naval Research. Critical readings of the manuscript by Professor Allan D. Pierce of MIT, as well as by Dr. David Feit and Dr. Miguel C. Junger of Cambridge Acoustical Associates, are gratefully acknowledged. The authors have also benefited from discussions with Robert M. Barash and Ira M. Blatstein, both of the U. S. Naval Ordnance Laboratory, White Oak, Silver Spring, Maryland.

* Present address: Dep. Music, Brandeis Univ., Waltham, Mass.

[1] R. M. Barash and J. A. Goertner, "Refraction of Underwater Explosion Shock Waves: Pressure Histories Measured at Caustics in a Flooded Quarry," U. S. Naval Ordnance Lab., Tech. Rep. 67-9 (19 Apr. 1967).

[2] C. B. Officer, *Introduction to the Theory of Sound Transmission* (McGraw–Hill, New York, 1958), pp. 96, 180–184.

[3] L. M. Brekhovskikh, *Waves in Layered Media* (Academic, New York, 1960), Chaps. 4 and 6.

[4] P. Hirsch, "Acoustic Field of a Pulsed Source in the Underwater Sound Channel," J. Acoust. Soc. Amer. **38**, 1018–1030 (1965).

[5] I. Tolstoy, "Total Internal Reflection of Pulses in Stratified Media," J. Acoust. Soc. Amer. **37**, 1153–1155 (1965).

[6] I. Tolstoy and C. S. Clay, *Ocean Acoustics: Theory and Experiment in Under-Water Sound* (McGraw–Hill, New York, 1966), pp. 58–61 and Chap. 5.

[7] A. O. Williams, Jr., and W. Horne, "Axial Focusing of Sound in the SOFAR Channel," J. Acoust. Soc. Amer. **41**, 189–198 (1967).

[8] I. Tolstoy, "Phase Changes and Pulse Deformations in Acoustics," J. Acoust. Soc. Amer. **44**, 675–683 (1968).

[9] Y. A. Kravtsov, "Two New Asymptotic Methods in the Theory of Wave Propagation in Inhomogeneous Media," Sov. Phys. Acoust. **14**, 1–17 (1968).

[10] I. Kay and J. B. Keller, "Asymptotic Evaluation of the Field at a Caustic," J. Appl. Phys. **25**, 876–883 (1954).

[11] C. Chester, B. Friedman, and F. Ursell, "An Extension of the Method of Steepest Descents," Proc. Camb. Phil. Soc. **54**, 599–611 (1957).

[12] D. Ludwig, "Uniform Asymptotic Expansions at a Caustic," Commun. Pure Appl. Math. **19**, 215–250 (1966).

[13] J. B. Keller and B. D. Seckler, "Geometrical Theory of Diffraction in Inhomogeneous Media," J. Acoust. Soc. Amer. **31**, 192–205 (1959); "Asymptotic Theory of Diffraction in Inhomogeneous Media," J. Acoust. Soc. Amer. **31**, 206–216 (1959).

[14] F. G. Friedlander, *Sound Pulses* (Cambridge U. P., Cambridge, England, 1958), p. 56.

[15] I. M. Blatstein, J. Acoust. Soc. Amer. (to be published).

[16] R. H. Cole, *Underwater Explosions* (Princeton U. P., Princeton, N. J., 1948), p. 239; and A. B. Arons, "Underwater Explosion Shock Wave Parameters at Large Distances from the Charge," J. Acoust. Soc. Amer. **26**, 343–346 (1954).

[17] A. Silbiger, "Focusing of Sound and Explosive Pulses in the Ocean," Cambridge Acoust. Ass., Inc., Tech. Rep. U-286-188, ONR Contr. N00014-66-C-0110 (June 1968).

[18] D. A. Sachs, "Underwater Shockwave Focusing at Caustics: Comparison of Theory and Experiment," Cambridge Acoust. Ass., Inc., Tech. Rep. U-322-188, ONR Contr. N00014-66-C-0110 (Aug. 1969).

[19] See, for example, G. F. Carrier, M. Krook, and C. E. Pearson, *Functions of a Complex Variable* (McGraw–Hill, New York, 1966), pp. 366–367.

[20] See, for example, Ref. 3, pp. 243–244.

[21] See, for example, K. G. Budden, *Radio Waves in the Ionosphere* (Cambridge U. P., Cambridge, England, 1966), Chap. 9.

[22] Ref. 3, pp. 245–250.

[23] D. H. Wood, "No Phase Change in a Constant Gradient Medium," J. Acoust. Soc. Amer. **44**, 1154–1155 (1968).

[24] R. M. Barash, "Evidence of Phase Shift at Caustics," J. Acoust. Soc. Amer. **43**, 378–380 (1968).

[25] For an introduction to asymptotic series, see P. M. Morse and H. Feshbach, *Methods of Theoretical Physics* (McGraw–Hill, New York, 1953), Part I, pp. 434–437.

[26] Examples of the application of asymptotic series are given by T. B. A. Senior, "Analytical and Numerical Studies of the Back Scattering Behavior of Spheres," Univ. Mich., Tech. Rep. 7030-1-T, AF Contr. 04(694)-683 (June 1965).

[27] C. L. Pekeris, "Theory of Propagation of Sound in a Half-Space of Variable Sound Velocity under Conditions of Formation of a Shadow Zone," J. Acoust. Soc. Amer. **18**, 295–315 (1946).

[28] Ref. 3, pp. 492–496.

[29] A. J. Friedman, "Phase Variation of the Acoustic Field Along a Ray," J. Acoust. Soc. Amer. **45**, 306(A) (1969). Friedman independently studied the asymptotic behavior of the field associated with the bilinear profile.

[30] Ref. 3, pp. 492–496.

[31] M. K. Myers and M. B. Friedman, "Focusing of Supersonic Disturbances Generated by a Slender Body in a Non-Homogeneous Medium," Columbia Univ., Dep. Civil Eng. and Eng. Mech., Tech. Rep. No. 40, Contr. Nonr-266(86) (June 1966).

[32] B. F. Cron and A. H. Nutall, "Phase Distortion of a Pulse Caused by Bottom Reflection," J. Acoust. Soc. Amer. **37**, 486–492 (1965).

[33] P. M. Morse and K. U. Ingard, *Theoretical Acoustics* (McGraw–Hill, New York, 1968), p. 282, Eq. 6.4.22; and F. R. Norwood, "Propagation of Transient Sound Signals into a Viscous Fluid," J. Acoust. Soc. Amer. **44**, 450–457 (1968), Eq. 1.

[34] Ref. 3, pp. 270–280.

[35] R. H. Lang and J. Shmoys, "Lateral Waves on Diffuse Interfaces of Finite Thickness," J. Acoust. Soc. Amer. **48**, 242–252 (1970).

[36] I. M. Blatstein, "Refraction of Underwater Explosion Shock Waves: A Method for Prediction of Pressures at Caustics," U. S. Naval Ordnance Lab., Tech. Rep. 69–181 (16 Jan. 1970).